

The paper is devoted to the development of new equipment for the production of metal-polymer thread. 3D printing with metal-polymer thread is one of the advanced directions in the technology of manufacturing metal parts of complex shape. The proposed technology is an alternative to the currently existing metal injection molding (MIM) technology and selective laser melting printing technology. An important step in this work was to conduct computational experiments to determine the effect of screw rotation on the process pressure parameter and the design of the main assembly of the screw extruder. As a result of the research, the pressures on the metal-polymer composition were determined depending on the rotation speed of the screw. With a rotation of 30 rpm, the pressure reached 0.05 Pa and the maximum pressure was 0.18 MPa. The experiments were carried out in the CradelSFlow program. The computer calculation showed a margin of the screw strength coefficient $k=1.8$, and a maximum deflection of $2.8 \cdot 10^{-4}$ m, which meets the condition of static rigidity. To determine the correct value of the gap δ between the screw ridge and the extruder walls, an analysis of the rotor dynamics was carried out. The result of this study is the critical extruder rotation speed of 60 rpm at which the phenomenon of precession may occur. Amplitude-frequency characteristics $y_{din}=7 \cdot 10^{-4}$ m. According to the results of the dynamic calculation, the screw dimensions were adjusted, the geometry was reduced by $\Delta=0.5$ mm. The experiments made it possible to verify the optimal parameters of the technological process of metal-polymer mixture extrusion. The data obtained are important for the improvement and development of 3D printing technology for metal parts of complex geometric shape

Keywords: feeder, extruder, computer simulation, pressure, gap, rotary dynamics

DEVELOPMENT OF THE DESIGN AND TECHNOLOGY OF EXTRUSION OF METAL-POLYMER MIXTURES FOR THE PRODUCTION OF FEEDSTOCKS

Madina Isametova

Candidate of Technical Sciences, Associate Professor*

Bakhyt Absadykov

Doctor of Technical Sciences, Professor,
Correspondent member of National Academy
of Science of the Republic of Kazakhstan*

Bauyrzhan Bazarbay

Correspondent author

Doctoral Student*

E-mail: bauyrzhan_4@mail.ru

Gulbarshyn Smailova

Candidate of Technical Sciences, Associate Professor*

*Department of Mechanical Engineering,
Standardization, Certification and Metrology
Satbayev University

Satpaev str., 22 a, Almaty,
Republic of Kazakhstan, 050013

Received date 31.05.2022

Accepted date 25.07.2022

Published date 31.08.2022

How to Cite: Isametova, M., Absadykov, B., Bazarbay, B., Smailova, G. (2022). Development of the design and technology of extrusion of metal-polymer mixtures for the production of feedstocks. *Eastern-European Journal of Enterprise Technologies*, 4 (1 (118)), 23–33. doi: <https://doi.org/10.15587/1729-4061.2022.259532>

1. Introduction

The development of production is based primarily on the application of advanced technologies. In [1], 10 such technologies were identified, among which additive and metal injection molding (MIM) technologies occupy the 1st and 2nd places, respectively. Until recently, a significant limitation to the use of MIM technology was the high cost of manufacturing parts in single and small batch production.

Currently, selective laser melting (SLM) is the only additive metal fabrication technology that has proven itself for industrial applications. The main disadvantage of this technology is the high cost of equipment. This problem holds back the development of 3D printing on metal. A promising direction is the printing of metal-polymer filament products on 3D printers that implement deposition modeling (FDM printers).

Printing uses a filament, which is a mixture of metal powder with a polymer that acts as a binder. After printing, the

product is thermally or chemically removed from the binder and sintered in an oven. In this case, the product is reduced in volume by 15–20 %. The implementation of this method is possible on inexpensive FDM printers, the cost of which is three orders of magnitude lower than that of SLM printers. The first experiments to test this technology began only in 2018, and at the moment almost all of them are conducted on filaments from BASF, whose product line consists of only one material, Ultrafuse 316 LX. At the same time, in the future, this technology will allow making parts not only of steel, but also of non-ferrous alloys, hard alloys, ceramics, etc.

The peculiarity of MIM technology and alternative technologies for manufacturing parts from metal polymers is that the blanks produced at a certain stage significantly affect the quality of the subsequent part. Thus, an error at any stage leads to a defective finished part. Therefore, it is necessary to control not only the process, but also the quality of blanks at intermediate stages. Therefore, the research carried out in the work is relevant and necessary for the development of

alternative more economical technologies, such as 3D printing with a metal-polymer thread.

2. Literature review and problem statement

Over the past few years, there has been a sharp increase in publication activity in the field of FDM printing using composite materials. Basically, the authors are trying to solve two problems – to find a cheap alternative to selective laser melting (SLM) technology, the cost of equipment for which starts from \$1 million and printing functional products from polymer-modified powders to give them special physical and mechanical properties, such as high hardness and wear resistance, electrical conductivity, photo-catalyst properties, high tensile, compression and bending strength [2–5].

In the literature, there is a considerable number of alternative MIM technologies and equipment, as well as an analysis of their parameters [6, 7]. For example, such equipment for 3D printing was proposed by the author [7]. The design of an extruder for a 3D printer that mixes metal polymer components – basis and hardener, feeds the composition into the printing zone and stacks, and after work has the ability to clean the mixing chamber for reuse.

For example, in [6] the influence of the diameter parameter of the extruder cutting disc was studied. With an increase in the diameter parameter of the cutting disc, the molding quality is gradually improved. The larger the diameter of the cutting disc, the better the molding quality of the extrudate. With a diameter of 7.5 mm, the surface of the mass is smooth. Based on these studies, a metal component with a complex three-dimensional structure, dense microstructure, excellent metallurgical adhesion and a flat surface was manufactured.

Despite the originality of the equipment, the author does not provide an analysis of the mutual influence of design and technological parameters on the structure of the green part.

In [7], the authors described an extruder for laying fast-setting two-component materials, described the process of degassing the extruded material, but did not mention the process parameters of obtaining a filament, such as the pressure in the extruder, optimal rotation speed of the screw and how these parameters will affect the quality of the extrudate.

In [8], a laboratory twin-screw mixer was used to mix binder and powder components in the manufacture of feed-stock. The thread was pulled on a laboratory press through a specialized die. At the outlet of the die, the thread was cooled by running water in an inclined trough, which excluded its stretching and allowed to obtain a thread of constant diameter. The diameter of the pulled thread was 1.75 mm. The method is distinguished by its novelty, but the paper did not focus on the mixing parameters of the metal-polymer mixture, and the quality of the thread was not evaluated from the extrusion parameters.

The author [9] was faced with the task of developing and manufacturing an extruder for the production of metal-polymer filament for FDM printing. Extruders for creating plastic thread exist, but they are ineffective. The researcher gave the sequence of the extruder design. The main distinguishing feature of the developed extruder from the existing ones is the design of the cooled screw, which will avoid jamming of the screw due to clogging of the channels with the material. Since the extruder is designed to produce a filament consisting of polymer and metal powder, the screw must have increased wear resistance to avoid abrasion. To solve this

problem, it is planned to apply a ceramic coating on it by the gas-flame method. The disadvantage of this study is that the author does not justify the thickness of the coating to be applied, which must be selected based on static and dynamic analysis of the screw rotation, where the main boundary condition will be the screw rotation speed.

The issues of designing the extruder and the technological process were given in [10–12]. The results of the study concerned equipment and processes related to polymer materials, and the cases of mixtures with metal inclusions were not considered.

In [10], a theoretical window of optimal extrudability was determined in terms of temperature, shear rate, and powder loading. But the screw rotation and pressure parameters were not mentioned, which directly affect such an indicator as the density of the extrudate.

The paper [11] presents the results of a study on the manufacture of metal-polymer filament and describes the stage of extrusion. A single-screw Brabender Plasti-Corder extruder was selected for the production of threads from composite material. The authors pointed out that the geometric dimensions of the matrix resist the flow, pressure is required to push the material through the matrix, but what dependencies describe the relationship of the geometric parameters of the matrix, rotation speed and pressure are not given.

The authors [12] considered the issues of viscous heating, which depends only on the screw speed and the concentration of recycled polypropylene. For a conventional screw design, the drum temperature, screw speed and two polypropylene mixtures with very different melt viscosity were selected as independent factors, while the melt pressure, mass productivity, screw torque and temperature increase in the matrix due to shear heating were dependent reactions. The interrelation of these factors was evaluated, but the interrelationships of technological factors with constructive factors, such as the die design and the pressure created in the extrudate, were not given.

In the developed methods for designing extruders, there is no research on the influence of technological parameters on the design of the geometric dimensions of the extruder.

So in [13], the main purpose of the strength calculation of the extruder is to find such optimal design parameters (geometric characteristics, control parameters) that, along with strength characteristics, would ensure a reduction in the overall material consumption of the structure. The work determines the strength of the screw, without taking into account the parameters of the rotor dynamics of the screw on its geometric dimensions.

The above papers do not study the simultaneous effect of the screw speed parameter, both on the design and on the extrudate pressure. However, as our own experience in creating equipment for the production of filament from the metal-polymer mixture has shown, the identification of the relationship between technological and design parameters at the design stage is necessary for the rational production of equipment and the choice of technological parameters of the production of extruded mixture for further production of high-quality filament for 3D printing of metal products.

3. The aim and objectives of the study

The aim of the work is to design an extruder for manufacturing metal-polymer filament for FDM printing on the basis

of identifying the impact of dynamic parameters of screw rotation on its design. This will make it possible to increase the efficiency of the extrusion process at the design stage.

To achieve the aim, the following objectives were set:

- to conduct numerical experiments to find the correlation between the angular velocity of screw rotation and pressure in the extrudate;

- to estimate the strength of the screw of the designed equipment for the production of pellets;

- to evaluate the influence of dynamic parameters of screw rotation on its design;

- to carry out experimental research to confirm the method of evaluating the influence of screw rotation parameters on the technological indices of the metal-polymer mixture extrusion process.

4. Materials and methods

4.1. Material and equipment

For the development of filament composition for the 3D printer, we chose the feedstock steel 316 LW from BASF as a basic component. The typical chemical composition of parts after sintering and basic characteristics of the feedstock are shown in Table 1, respectively.

Table 1

Parameters of feedstock 316LW

Parameter	Unit of measure	Standard values	Special values	Test method
MFI	g/10 min	950	300–1,300	ISO 1133 (1900C.21.6 kg)
Density	g/m ³	7.9	≥7.95	ISO 3369
Out-of-size	–	1.1669	1.1629–1.1710	RC/PQ-SH-1360

A continuous press device was designed and modeled for the production of feedstock from a metal-polymer mixture. This device for manufacturing long profiles from powder materials contains a hopper of initial materials (feedstock), drive, heated cylinder, screw, fixed and movable plate, static screw-shaped mixer, hydraulic cylinders of the drive of press-stamp movement [14]. Fig. 1 shows a computer model of the new press device.

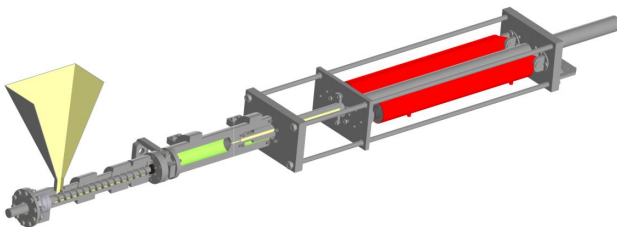


Fig. 1. 3D model of the press device

In the first stage of the design, the basic geometric parameters of the screw and cylinder were determined. The extrusion chamber is divided into three zones: feeding, compression, dosing. The depths of the channels in each zone were determined, as well as the dimensions of each zone. The screw pitch, angle and thickness of the coil were calculated. The maximum output of the extruder was pre-calculated to

be approximately 2.5 kg/h. The required screw speed as well as the approximate torque were calculated. Based on these data, a gear motor was selected to drive the screw with the possibility of adjusting the speed using a frequency converter. The heating elements (3 ceramic heaters for each zone and one for the nozzle) are selected. The main distinguishing feature of the designed extruder from the existing ones is the replaceable screw static mixer at the end of the extruder to create a prepressing effect [14].

Main parameters of the extruder:

- screw diameter $D_s=30$ mm;

- screw length $L=565$ mm;

- feed zone $L_f=0.25$, $L=0.25 \times 565 = 141$ mm;

- compression zone $L_p=0.35$, $L=0.35 \times 565 = 175$ mm;

- dispensing area $L_d=160$ mm;

- barrel diameter $D_b=D_s+2\delta=30.3$ mm, where δ is the clearance, $\delta=0.005$, $D_s=0.3$ mm.

Channel depth:

- in the feed zone $h_1 \approx 0.12D \approx 3$ mm;

- in the dosing zone $h_3 \approx 3/\text{compression ratio} = 3/4 = 0.75$ mm;

- screw step: $t \approx D_s = 30$ mm;

- coil thickness: $e \approx 0.1$, $D=3$ mm.

4.1.1. Modeling the technological process of extrusion

As mentioned above, the quality of the intermediate stages of the metal-polymer production process will affect not only the properties of the finished products. The extrusion process is significantly influenced by the pressure created by the screw. This parameter affects the processing temperature of the mixture and the quality of the extrudate obtained, and the operation of the extruder. The main parameters determining the quality of the feedstock are density, viscosity stability, and the required dependence of viscosity on shear rate. Failure to match the density and viscosity of the feedstock results in an unstable flow regime during filling and does not allow controlling the quality of the pellet [15].

In order to find the extruder's extrusion pressure, the movement of the material through the annular conical channel of the die is considered according to the diagram shown in Fig. 2. The gap for the passage of the material is formed by the tapered surface of the die and the tapered surface of the shaft.

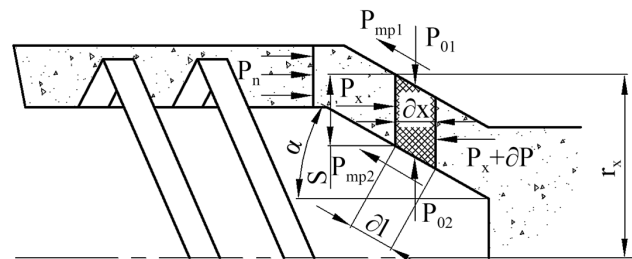


Fig. 2. Material movement in the extruder

For an elementary section of thickness dx , the differential equation of equilibrium with respect to the horizontal axis X has the form [16]:

$$Px\pi(2Srx - S2) - (Px + dP)\pi(2Srx - S2) - Ftr1 - Ftr2 = 0, \quad (1)$$

where P_x – pressure at the current channel section, Pa; $Ftr1$, $Ftr2$ – friction forces on the die wall and the shaft, respectively, N.

The expression for the value of the current pressure in differential form is as follows:

$$-\frac{dP}{P_x} = \frac{2\xi r' \cos \alpha}{S} dx. \tag{2}$$

Solving equation (2) by integration with boundary conditions from 0 to 1, the final equation for finding the pressing pressure:

$$P_n = \frac{P_0}{e^{\frac{2\xi r' l \cos \alpha}{S}}}, \tag{3}$$

where P_n is the pressure at the outlet of the orifice, Pa.

The pressure in the extruder was determined numerically by the finite volume method implemented in the CradelSFlow program. Fig. 3 shows a screw pair with a small domain. The boundary conditions for the numerical experiment are given in Table 2.

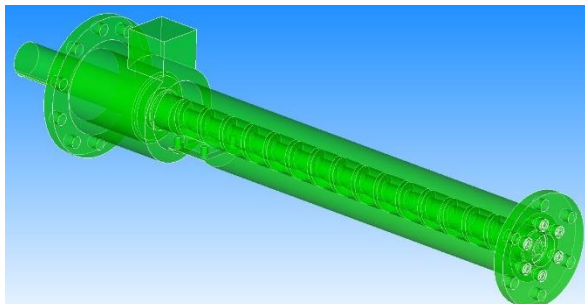


Fig. 3. Extruder model for the finite volume method

Table 2

Boundary conditions for technological calculation

Parameter	Value
Screw angular speed	30÷130 in increments of 40
Polymer metal density	7.9 kg/m ³
Modulus of elasticity, E	2·10 ⁵ MPa
Poisson's coefficient	0.3
Temperature	180

To simulate the process, a small domain for the screw was built. The domain and screw were divided into finite volumes, and the model consisted of 35,000 volumes.

The assumptions used for the screw extruder flow analysis are summarized as follows [16]:

- the flow regime in the screw extruder is laminar;
- the composite melt is an incompressible fluid;
- viscosity is modeled as a function of temperature and shear rate;
- the thermal regime between the screw surface and the polymer melt is adiabatic;
- a no-slip condition is imposed on a continuous boundary;
- density and specific heat are constant;
- the cylinder is completely filled with polymer melt;
- sustainable flow of polymer melt is achieved after the screw has made a sufficient number of revolutions.

4. 2. Static calculation of the screw

For the evaluation of the strength properties of an extruder, we consider the screw, which is the most heavily

loaded part of the extruder. The main objective of strength calculations for an extruder is to find optimum design parameters (geometric characteristics, control parameters) that, along with strength characteristics, would reduce the overall material intensity of the design. The design of screws does not take into account the strength characteristics of their elements. However, due to the longitudinal-transverse bending of the screw axis, premature wear of the outer cylinder and failure of the screw are possible [17]. The strength of the screw is determined taking into account the action of torsional and bending moments on its axis. In most cases, the strength calculation of this kind of structures is carried out by a simplified method, which takes into account only the deformation from bending with torsion. But in our case of the screw design, there is also a longitudinal force from the pressure of the material as it leaves the matrix. Therefore, we carry out the calculation considering the bending deformation. The maximum stresses arising in the screw sections at longitudinal-transverse bending are determined by the formulas:

$$\sigma_{\max} = \frac{4N \cdot (1 + \alpha^4) + \pi y \cdot l^2 \cdot D \cdot (1 - \alpha^4)}{\pi \cdot D^2 \cdot (1 - \alpha^4)}, \tag{4}$$

where σ_{\max} – maximum design normal stress, MPa; N – longitudinal force from the extrudate pressure.

The tangential stress is equal to:

$$\tau_{\max} = \frac{16 \cdot M_{kp}}{\pi \cdot D^3 \cdot (1 - \alpha^4)}, \tag{5}$$

where τ_{\max} – tangential stress, MPa; M_{kpn} – torque, kH·m.

Theoretical calculation of screw deflection, based on the elastic line equation:

$$EI_x \frac{d^2 \cdot y}{d \cdot x^2} = M_x, \tag{6}$$

where E – Young's modulus, MPa; I_x – axial moment of inertia of the section, m⁴; M_x – bending moment relative to the transverse axis, kH·m.

The deflection equation takes the following form:

$$\Gamma = \frac{1}{E_j} \cdot \left\{ \begin{aligned} & \left[\frac{q}{k^2} \cdot \left(\frac{1}{k^2} + \frac{L^2}{2} \right) - \right. \\ & \left. - \frac{1}{k} \cdot \left[\frac{q}{k^3} + q \cdot \left(L - \frac{1}{k} \cdot \sin kL \right) \cdot \cos kL \right] \right] - \\ & \left. - \frac{1}{k^2} \cdot \left[\frac{qL}{k} - q \cdot \left(L - \frac{1}{k} \cdot \sin kL \right) \cdot \sin kL \right] \right\}. \tag{7}$$

The screw itself has a rather complex configuration, so further analysis of its strength characteristics by the analytical method will not be accurate enough. To solve the problem, we used the finite element method implemented in the integrated system NASTRAN. Fig. 4 shows a drawing of the screw.

The mechanical design includes the boundary conditions listed in Table 3.

To evaluate the quality of the mesh, we used the method from [18]. The density of the mesh or the degree of element refinement is one of the most important parameters to control the accuracy of the solution (the chosen type and shape of the elements are of course also important).

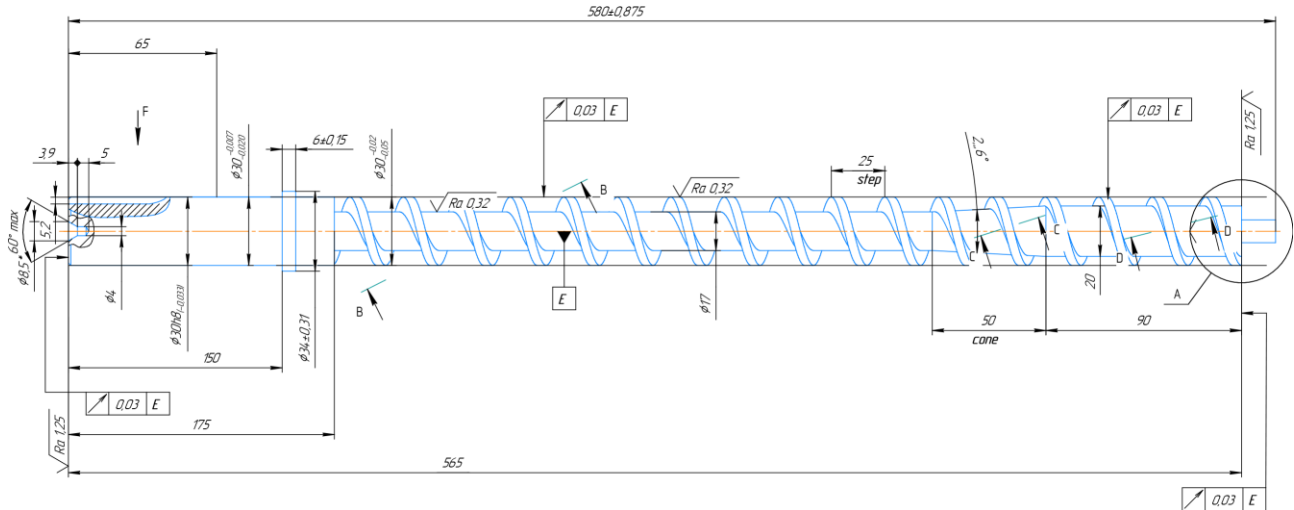


Fig. 4. Drawing of the screw

If there are no singularities in the model (sharp angles, loads and fixations applied at a point, etc.), a finer mesh will give a more accurate result. Nevertheless, a large number of elements in a fine mesh will require more costs in terms of computing station memory and computation time. One of the ways to assess the quality of a grid (and a model as a whole) can be the verification of calculation results with the help of experimental data or analytical solutions. Unfortunately, they are not always available to the user, if at all. Thus, other methods of quality assessment have found application in engineering practice. These include consistent mesh refinement, as well as interpolation of jumps in the values of the results.

Table 3

Boundary conditions for dynamic analysis

Parameter	Value
Longitudinal force	$N(P)$ is determined from the technological calculation
Own weight of the screw	20 H
Modulus of elasticity, E, of the screw material	$2.1 \cdot 10^5$ MPa
Poisson's coefficient	0.3

The basic and most accurate method of assessing mesh quality is to decrease the size of the elements successively until some significant result, such as the maximum stress in a certain zone, converges to a certain value (that is, with each iteration the stress change is less than a given tolerance). Fig. 5 shows that increasing the grid density first leads to a sharp increase in the maximum stress, but then the rate of increase slows down greatly and finally the curve reaches a nearly horizontal «shelf», where a large increase in grid density corresponds to only a small change in the maximum stress.

The starting and ending points of this plot in this case can be considered points with densities of 115,000 and 297,650 elements per unit area. When you change the density by a factor of four, the value of the analyzed result increased only by 1.5 %. Fig. 6 shows the finite element model of the screw.

When discretizing the model, 297,650 elements were generated, the problem was solved in the solver Solver120, the settings of the solver Cassio made it possible to reduce the counting time.

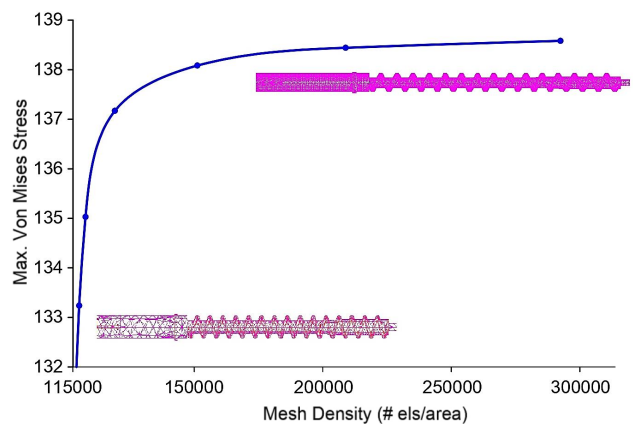


Fig. 5. Mesh quality



Fig. 6. Finite element model of the screw

4. 3. Dynamic calculation of the screw

Ensuring the required clearance between the screw coils and the housing in the sealing zone allows the extruded material to be degassed. The gap δ between the screw coils and the housing in the sealing zone is selected from the condition of zero flow of the extruded material through the annular gap and is determined by the formula [19]:

$$\delta = \sqrt{\frac{6V_{st} \cdot \mu \cdot L}{\pi \cdot D \cdot \Delta P}}, \quad (8)$$

where V_{st} – speed of movement of the screw wall forming the gap relative to the cylinder, μ – coefficient of dynamic viscosity of the extruded material, L – width of the screw, D – diameter of the hole in the housing, ΔP – differential pressure under which the fluid flows.

According to the calculated (8), the clearance for our equipment is $\delta = 0.3$ mm. During the first adjustment of the equipment, jamming of the screw occurred, which caused the need to study the effect of screw rotation on its deflections.

The rotor dynamics of the screw was analyzed in NAS-TRAN/ROTORDYNAMICS to compare the static and dynamic gap between the screw coils and the extruder wall. The

screw was modeled with 20 bar beam elements (Fig. 7) and the boundary conditions for the analysis are given in Table 4.

Table 4

Boundary conditions for the analysis of the rotor dynamics of the screw

Parameter	Value
Screw material density	7,800 kg/m ³
Modulus of elasticity, E	2·10 ⁵ MPa
Poisson's coefficient	0.3
Screw rotation speed	150 rpm

To determine the frequencies of the perturbed oscillations we use the COMPLETE SOLUTION (complex frequencies) solver. You can use the asynchronous processing option (ASYNC) in the program to determine the response of the system to an external action that does not depend on the rotation speed. With the synchronous precession option (SYNC), the system response to unbalance or other excitation, which depends on the rotor speed, is determined.

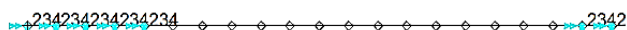


Fig. 7. Model of a beam screw

The beam model consists of 20 elements. The ASYNC solver was used. By means of complex shape analysis, we can determine the frequencies of oscillations corresponding to the forward and reverse precession, as well as the critical speeds of rotation [20].

To assess the deformation of the screw caused by the centrifugal force from the unbalance of the rotor, we will study the amplitude of the forced vibrations from the unbalance force of the screw. For this purpose, a periodic force applied to the center of mass of the screw is specified. As a result of the solution, the deformations of the screw at various rotation frequencies will be obtained. The analysis will be performed in the NASTRAN solver 122.

5. Results of the study of the design and technology of extrusion

5.1. Results of the study of the effect of the screw rotation speed on the pressure in the extrudate

The results of the process study are shown in Fig. 8 as diagrams of pressure distribution in the extruder cylinder cavity.

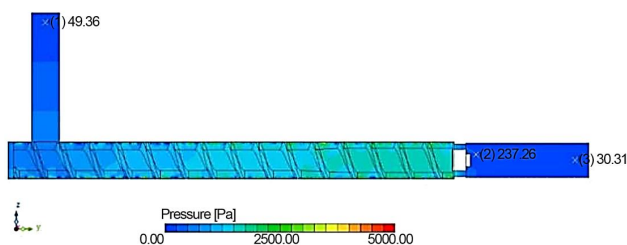


Fig. 8. Pressure distribution at a speed of 30 rpm

The pressure charts show the maximum pressure in the extruder at 1 MPa at a speed of 70 rpm, and the color charts

along the cylinder cavity show the pressure increase as the screw speed increases. The maximum pressure drop in the compression zone is $\Delta P=0.95$ Pa. The determined values will be used as input data for the strength calculation and calculation of the dynamic gap between the screw coils and the extruder cylinder walls.

5.2. Results of the influence of pressure in the extrudate on the strength and rigidity of the screw

The results of the static calculation are presented in the form of stress and strain diagrams in Fig. 9.

The diagrams shown in Fig. 6 indicate dangerous sections in the screw support area, stress and strain isolines indicate that the contribution of torque to the stress-strain state of the screw is dominant.

According to the diagram, the maximum stress in the screw sections $\sigma_{max}=139$ MPa, maximum movement $Y_{max}=6.58 \cdot 10^{-5}$ m. The analysis shows sufficient safety factor $k=1.7$, the maximum deflection satisfies the stiffness condition $Y_{max} < L/200$, L – length of the screw.

5.3. Results of the study of the rotor dynamics of the screw and its influence on the design parameters of the screw

The results of the rotor dynamics study are the rotor waveforms shown in Fig. 10 and the Campbell diagram shown in Fig. 11.

According to the Campbell diagram, the first resonant velocity is $\omega_c=58$ rpm, intersection of the second multiplicity line with the lowest natural frequency. As a result of the analysis of the frequency response of the solution, the deformations of the screw at different frequencies of rotation are obtained. Fig. 12 shows the dependence of the amplitude of forced vibrations of the screw on the rotation speed.

The node in the middle of the screw was selected for the frequency response analysis. The diagram in Fig. 10 shows the appearance of 2 harmonics at a frequency of 1 Hz and 3 Hz, the resonance phenomenon occurs at a frequency of 1 Hz and the vibration amplitude takes the value $Y_{max}=6 \cdot 10^{-4}$ m.

Fig. 13 shows a transient diagram of the unbalance force at a frequency of 1 Hz, defined from the Campbell diagram as critical.

Maximum peaks of amplitude $Y_{din}=7 \cdot 10^{-4}$ m, which agrees with the amplitude-frequency characteristic presented in Fig. 12.

5.4. Experimental investigation of the effect of screw speed on extrudate density

Experimental studies were performed with the equipment after adjustment and adjustment of the screw geometry. A tolerance has been removed from the coils $\Delta=0.4$ mm equal to the difference between the resonant value of the screw movement and the static value of the gap $\delta=0.3$ mm. Fig. 14 shows the adjusted screw.

The experiments were conducted in the extruder (Fig. 15), at a temperature of 1,500 – zone of delivery, 1,700 – zone of compression and 1,800 – zone of dosing.

To record the processes occurring in the extruder and the subsequent comparison of experimental and theoretical dependences, first of all, on the pressures developed, a strain gauge unit was created. The sequence of experiments was carried out on the basis of known planning methods for given response functions and controllable parameters, and the accuracy and adequacy of the results on the basis of regression analysis and statistical processing of the results.

Patran 2021 18-Jun-22 13:10:28

Fringe: SC1:DEFAULT, A1:Static subcase, Stress Tensor, , von Mises, (NON-LAYERED)

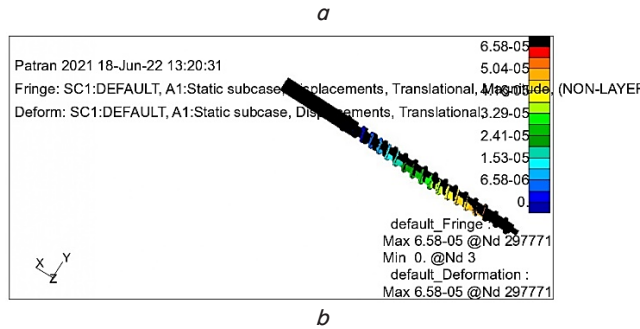
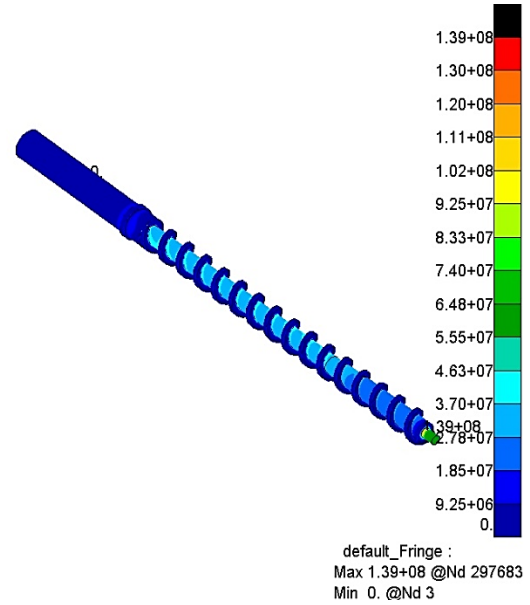


Fig. 9. Diagrams of: *a* – stresses; *b* – deformations

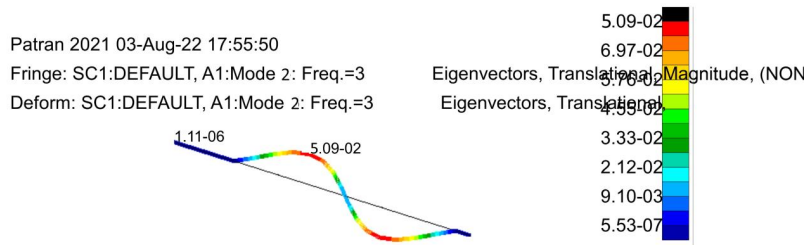


Fig. 10. Second form of oscillation

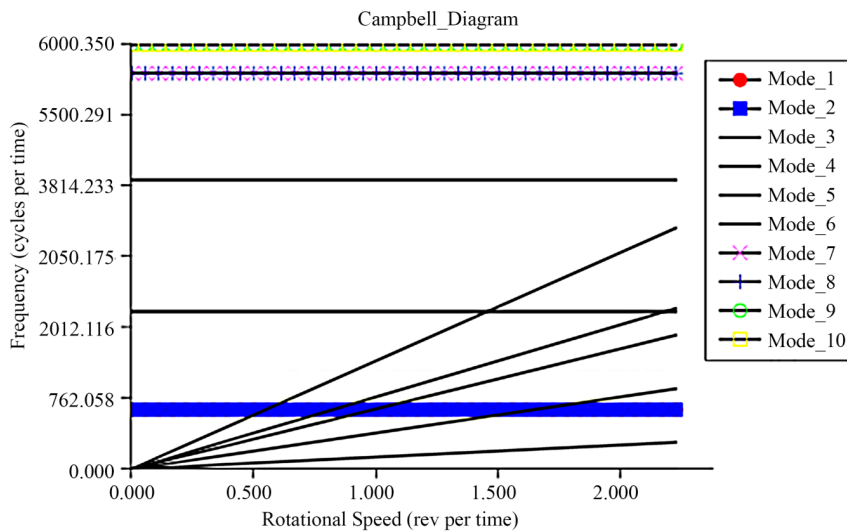


Fig. 11. Campbell diagram

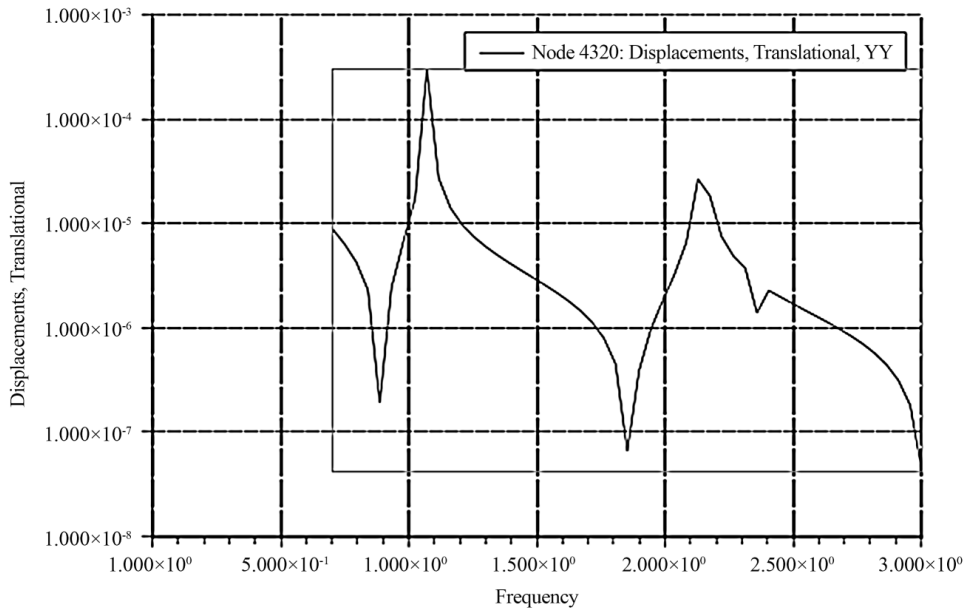


Fig. 12. Amplitude-frequency response of the screw at 3 Hz

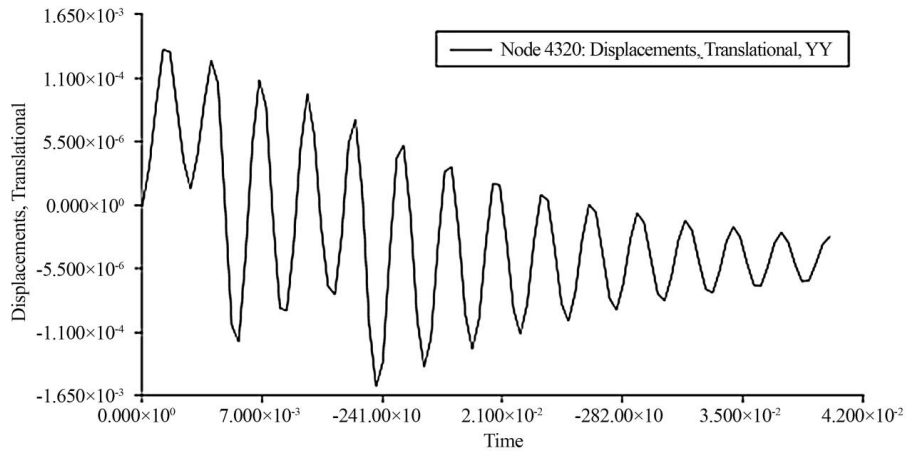


Fig. 13. Transient response from screw unbalance force at 1 Hz



Fig. 14. Adjusted screw

The screw speed was adjusted from 10 rpm to 120 rpm in 20 rpm increments, with the extruder running for about five minutes at each speed. To determine the effect of the pellet design, i.e. the hole size, on the extrudate pressure, pellets with hole diameters in the range of 5 to 10 mm were used.

The regression equation of the experimental results and their graphical representation are shown in Fig. 16.

$$P = 0.853 + 0.0065 \cdot D - 0.017 \cdot D^2 - 0.006 \cdot n + 0.003 \cdot n^2 - 0.0001 \cdot d \cdot n. \tag{9}$$



Fig. 15. Pressing device

By making sections of the presented three coordinate surfaces, we obtain two parametric plots of the pressure generated by the screw extruder on the diameter of the hole in the die D , on the screw revolution n .

From the graphs in Fig. 16, it is obvious that the pressure increases with the number of revolutions, and decreases with increasing hole diameters in the outlet die.

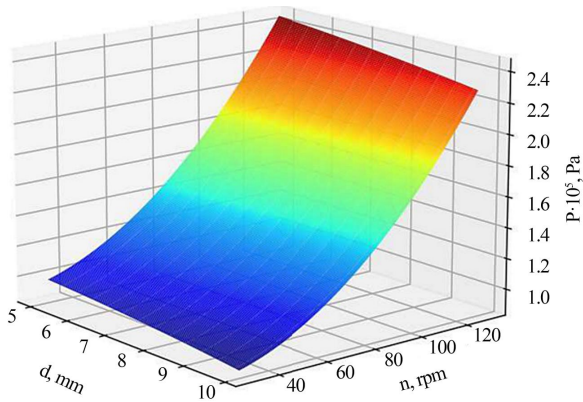


Fig. 16. Pressure function response surface from parameters n, d

The optimum values of P and n were determined experimentally. The density of the extrudate was measured according to GOST 56679-2015 by collecting and weighing the output data for 2 minutes. Results and discussion of the measured densities at each screw speed for both materials are shown below. The results of measuring the extrudate density are shown in Table 5. The visual picture of the experiment was also analyzed (Fig. 17).

Table 5

Results of extrudate density measurements

Screw rotation speed, rpm	Extrudate weight, kg	Extrudate density, kg/m ³
30	11.037	1,283
50	11.30	1,289
70	11.55	1,300
90	11.87	1,390



Fig. 17. Extruded flow

At 70 rpm, there was a smooth extrudate flow with no «stall» or flow instability.

6. Discussion of the results of designing an extruder for manufacturing metal-polymer filament

Numerical experiments to determine the pressure on the extrudate showed a direct dependence of the pressure parameter on the screw rotation speed. From the diagrams

in Fig. 8, the pressure distribution shows a directly proportional relationship between the pressure and the speed of the screw, and the change in the colors of the diagram indicates an increase in pressure in the area in front of the fan. This is due to the fact that an increase in the shear rate leads to a decrease in the initial humidity. The pressure in the pre-matrix zone of the extruder increases sharply due to the fact that a small amount of water during extrusion further increases the viscosity of the product. Therefore, it is important to take into account and optimize the geometric shape of the die and find the relationship between the distance indicators and, finally, the relationship between the screw rotation speed as an input parameter and the quality of the extrudate, estimated by the density of the mixture at the output.

The maximum pressure value is one of the parameters of the strength calculation, so the longitudinal force acting on the screw was calculated according to the formula $N = P_{max} \cdot S$, and applied to the output end. This boundary condition for modeling the stress-strain state distinguishes our study from the previously proposed methods, where the calculation of the screw is reduced to bending deformation from the applied pressure force of the extrudate. From the results of the strength calculation presented in Fig. 9, the sufficiency of the coefficient of safety margin $k = 1.8$ and the rigidity of the screw is obvious, but the practice has shown the insufficiency of fulfilling the condition of static rigidity of the screw $Y_{st} = 2.8 \cdot 10^{-4}$ m, since the first adjustment identified such a problem as jamming of the screw.

Research on the rotor dynamics of the screw and its influence on the design parameters of the screw indicates the occurrence of a critical rotation speed at a frequency of 1 Hz, in the Kemppbel diagram in Fig. 11. For harmonics of this frequency, according to Fig. 12, the maximum amplitude of the deviation from equilibrium is $Y_{din} = 7 \cdot 10^{-4}$ m, which exceeds the static deviation of $2.8 \cdot 10^{-4}$ m. According to the results of the dynamic calculation, the dimensions of the screw were adjusted, the geometry was reduced by $\Delta = 0.4$ mm.

Experimental studies on the effect of screw rotation speed on extrudate quality allowed us to derive a regression dependence (9) of pressure in the extruder on the speed and design of the die. The graphs 17 show a maximum pressure of 1.8 MPa at a speed of 140 rpm, and at the size of holes in the die $D = 5$ mm. A rational parameter for the screw rotation was chosen based on a visual inspection of the extrudate, so that at a speed of 70 rpm, the density of the extrudate was 1,300 kg/m³ and the flow had a smooth shape, which indicates the absence of the phenomenon of «disruption». The extrudate density was 1,300 kg/m³ and the flow was smooth.

The disadvantages of the conducted research are the insufficient number of experiments carried out due to the high cost of the material, the technological process is deeply stochastic and requires more tests for the correct regression equation. For this reason, the coefficients of the obtained regression equation may not have high accuracy.

7. Conclusions

1. Computational experiments were carried out with CradelSFlow to determine the pressure on the metal-polymer composition depending on the rotation speed of the screw. With a rotation of 30 rpm, the pressure reached 0.5 Pa and the maximum pressure was 1 MPa.

2. Using the results of technological calculation, we determined the longitudinal force acting on the end of the screw and created a design mechanical scheme to determine the strength of the screw. The results showed a safety factor of $k=1.8$, which indicates sufficient strength of the screw and the maximum deflection is $2.8 \cdot 10^{-4}$ m, which corresponds to the condition of static stiffness.

3. In order to determine the correct value of the gap δ between the screw crest and the extruder walls, the rotor dynamics were analyzed, resulting in a critical speed of 70 rpm, at which the phenomenon of precession might occur. To determine the amplitude of the screw deflection from the unbalance force, the amplitude-frequency characteristic was determined $Y_{din}=7 \cdot 10^{-4}$ m. Based on the results of the dynamic calculation, the screw dimensions were corrected, the geometry was reduced by $\Delta=0.4$ mm.

4. Experiments were carried out to determine the extrudate density at different screw speeds. The experiments allowed us to obtain a regression equation for the pressure function depending on the variables of rotation speed and die geometry. The optimum screw rotation parameter is

70 rpm, which satisfies the condition of screw rotation stability and the extrudate quality index, such as density and laminarity.

Conflict of interest

The authors declare that they have no conflict of interest in relation to this research, whether financial, personal, authorship or otherwise, that could affect the research and its results presented in this paper.

Acknowledgments

This research was supported by the research grants AP08857034 «Development of a new design of pressing equipment and a chamber with a gas-dynamic installation with program control for the manufacture of additive technology of high-quality products» from the Ministry of Education and Science of the Republic of Kazakhstan for 2020–2022.

References

1. Michaeli, W., Bielzer, R. (1991). Metal injection molding: Shaping sintered metal parts. *Advanced Materials*, 3 (5), 260–262. doi: <https://doi.org/10.1002/adma.19910030511>
2. Korotchenko, A. Yu., Khilkov, D. E., Tverskoy, M. V., Khilkova, A. A. (2020). Research of 3D Printing Modes of Feedstock for Metal Injection Molding. *Materials Science Forum*, 992, 461–466. doi: <https://doi.org/10.4028/www.scientific.net/msf.992.461>
3. Bazlov, V. A., Mamuladze, T. Z., Kharitonov, K. N., Efimenko, M. V., Golenkov, O. I., Pronskikh, A. A. et al. (2020). Capabilities injection molding of metal powders (MIM – metal injection molding) the production of medical products. *International Journal of Applied and Fundamental Research*, 2, 64–68. doi: <https://doi.org/10.17513/mjpf.13011>
4. Ewart, P. (2012). Metal Powder Injection Moulding, Research and Industry. A review and assessment of MIM as a commercial process and the barriers to successful manufacture. Available at: https://www.researchgate.net/publication/267271664_Metal_Powder_Injection_Moulding_Research_and_Industry_A_review_and_assessment_of_MIM_as_a_commercial_process_and_the_barriers_to_successful_manufacture
5. Parmatech: The MIM industry's first commercial producer, and still going strong (2010). Powder Injection Moulding International, 4 (2). Available at: <https://www.pim-international.com/wp-content/uploads/sites/2/2017/07/PIM-International-June-2010-DP.pdf>
6. Yan, X., Hao, L., Xiong, W., Tang, D. (2017). Research on influencing factors and its optimization of metal powder injection molding without mold via an innovative 3D printing method. *RSC Advances*, 7 (87), 55232–55239. doi: <https://doi.org/10.1039/c7ra11271h>
7. Chepchurov, M. S., Lubimyi, N. S., Chetverikov, B. S., Zubenko, I. N., Odobesko, I. A. (2019). Implementation of Additive printing using thermoset polymer materials and two-component printing mixture. *Additive Fabrication Technology*, 1 (1), 36–46.
8. Korotchenko, A. Y., Khilkov, D. E., Tverskoy, M. V., Khilkova, A. A. (2020). Use of additive technologies for metal injection molding. *Engineering Solid Mechanics*, 8, 143–150. doi: <https://doi.org/10.5267/j.esm.2019.10.001>
9. Roshchupkin, S. I., Golovin, V. I., Kolesov, A. G., Tarakhovskiy, A. Y. (2020). Extruder for the production of metal-polymer filament for additive technologies. *IOP Conference Series: Materials Science and Engineering*, 971 (2), 022009. doi: <https://doi.org/10.1088/1757-899x/971/2/022009>
10. Strano, M., Rane, K., Briatico Vangosa, F., Di Landro, L. (2019). Extrusion of metal powder-polymer mixtures: Melt rheology and process stability. *Journal of Materials Processing Technology*, 273, 116250. doi: <https://doi.org/10.1016/j.jmatprotec.2019.116250>
11. Masood, S. H., Song, W. Q. (2004). Development of new metal/polymer materials for rapid tooling using Fused deposition modeling. *Materials & Design*, 25 (7), 587–594. doi: <https://doi.org/10.1016/j.matdes.2004.02.009>
12. Fu, T., Haworth, B., Mascia, L. (2016). Analysis of process parameters related to the single-screw extrusion of recycled polypropylene blends by using design of experiments. *Journal of Plastic Film & Sheeting*, 33 (2), 168–190. doi: <https://doi.org/10.1177/8756087916649006>
13. Rauwendaal, C. (2014) Polymer Extrusion. Hanser, 950. doi: <https://doi.org/10.3139/9781569905395>

14. Absadykov, B. N., Mashekova, A. S. et. al. (2020). Pat. No. 35634. Continuous pressing device for producing long profiles from powdered materials. No. 2020/0905.1; declared: 31.12.2020; published: 06.05.2022, Bul. No. 18. Available at: <https://gosreestr.kazpatent.kz/Invention/Details?docNumber=335940>
15. Abdel-Ghany, W. E., Ebeid, S. J., Fikry, I. (2015). Effect of Geometry and Rotational Speed on the Axial Pressure Profile of a Single Screw Extrusion. *IJISSET – International Journal of Innovative Science, Engineering & Technology*, 2 (1). Available at: https://www.researchgate.net/publication/308209459_Effect_of_Geometry_and_Rotational_Speed_on_the_Axial_Pressure_Profile_of_a_Single_Screw_Extrusion
16. Kim, N., Kim, H., Lee, J. (2006). Numerical analysis of internal flow and mixing performance in polymer extruder I: single screw element. *Korea-Australia Rheology Journal*, 18 (3), 143–151. Available at: <https://www.cheric.org/PDF/KARJ/KR18/KR18-3-0143.pdf>
17. Zagoruiko, M. G., Vasilchikov, V. V., Mamakhai, A. K. (2020). Simulation of the Extruder Screw Parameters. *Agricultural Machinery and Technologies*, 14 (4), 71–77.
18. Isametova, M., Nussipali, R., Karaivanov, D., Abilkhair, Zh, Isametov, A. (2022). Computational and Experimental Study of the Composite Material for the Centrifugal Pump Impellers Manufacturing. *Journal of Applied and Computational Mechanics*, 8 (4), 1407–1421. doi: <https://doi.org/10.22055/JACM.2022.40366.3574>
19. Ojolo, S. J., Ajiboye, J. S., Orisaleye, J. I. (2015). Plug flow analysis for the design of the compaction region of a tapered screw extruder biomass briquetting machine. *Agric Eng Int: CIGR Journal* September, 17 (3). Available at: https://www.researchgate.net/publication/283844646_Plug_flow_analysis_for_the_design_of_the_compaction_region_of_a_tapered_screw_extruder_biomass_briquetting_machine
20. Isametova, M., Absadykov, B., Batyrgaliyev, M., Borovik, I. (2018). Centrifugal pump rotor dynamics study. *NEWS of National Academy of Sciences of the Republic of Kazakhstan*, 5 (431), 226–233. doi: <https://doi.org/10.32014/2018.2518-170x.29>